Inorg. Chem. **2003**, *42*, 2378–2383

Novel Titanium Compounds for Metal–Organic Chemical Vapor Deposition of Titanium Dioxide Films with an Ultrahigh Deposition Rate

Kyoungja Woo,*,† Wan In Lee,‡ Jong Seung Lee,‡ and Sang Ook Kang§

Nano-Materials Research Center, Korea Institute of Science and Technology, P.O. Box 131, Cheongryang, Seoul 130-650, Korea, Department of Chemistry, Inha University, Inchon 402-752, Korea, and Department of Chemistry, Korea University, 208 Seochang, Chochiwon, Chung-nam 339-700, Korea

Received May 6, 2002

A new titanium diolate compound Ti(mpd)(mdop)$_2$ (**1**) containing a β-ketoester and a dimeric derivative [Ti(mpd)(mdop)(μ-OMe)]$_2$ [**2**; mpd = 2-methyl-2,4-pentanediolate, mdop = $(CH_3)_3CC(O)C^-HCOOCH_3$] have been synthesized and characterized by FT-IR, ^{1}H NMR, ^{13}C NMR, mass spectroscopy, and elemental analysis. Complex **2** was further characterized by X-ray structural analysis. Both **1** and **2** are fairly stable in air and in solvents such as tetrahydrofuran and toluene. They are also thermally stable and do not leave any residue during flash evaporation at around 280 °C. The new titanium complexes were used as precursors for the deposition of TiO_2 thin films by liquid-source metal–organic chemical vapor deposition. Compared with commercial Ti precursors, such as Ti(mpd)(tmhd)$_2$ (tmhd = 2,2,6,6-tetramethylheptanedionate) and Ti(OPr^i)$_2$(tmhd)$_2$, the new titanium complexes demonstrated a much higher deposition rate of TiO_2 film growth (3–6 times) at 400–475 °C. The deposited TiO_2 film from complex **2** was found to be in a crystalline anatase phase with a smooth surface morphology and low carbon content. Crystal data for **2**: 233(2) K, a = 12.570(4) Å, b = 13.817(4) Å, c = 11.157(3) Å, β = 101.059(5)°, monoclinic, space group $P2_1/c$, Z = 2.

Introduction

Titanium is an important constituent of many metal oxides that have potential applications in microelectronic devices.[1−4] For instance, TiO_2 film has been studied as an alternative to SiO_2 in gate dielectrics of metal oxide semiconductor field effect transistors. Also, many Ti-containing composite materials, such as (Ba, Sr)TiO_3 (BST), Pb(Zr, Ti)O_3, $BaTiO_3$, $Bi_4Ti_3O_{12}$, etc., show promise as high dielectric and ferroelectric capacitor materials. Metal−organic chemical vapor deposition (MOCVD), because of its excellent step coverage, high deposition rate, and easy composition control,[5−7] has evolved as the method of choice for the mass production of thin films. The availability of a good Ti precursor for the MOCVD process is a prerequisite for the realization of new microelectronic devices that depend on TiO_2 films.

In this work, we have focused on the development of new Ti precursors applicable to the fabrication of a BST film. The BST film is thought to be the most promising material for dynamic random access memory (DRAM) capacitors because of its low-leakage current density, high dielectric constant, and easily controllable properties with the variation of the Ba/Sr composition ratio.[2,8−10] The commercial Ba and Sr precursors M(tmhd)$_2$·L and M(methd)$_2$ (M = Ba or Sr, tmhd = 2,2,6,6-tetramethylheptanedionate, L = pentamethyldiethylenetriamine or tetraglyme, methd = methoxyethox-

* Author to whom correspondence should be addressed. E-mail: kjwoo@kist.re.kr.
† Korea Institute of Science and Technology.
‡ Inha University.
§ Korea University.

(1) Campbell, S. A.; Gilmer, D. C.; Wang, X.-C.; Hsieh, M.-T.; Kim, H.-S.; Gladfelter, W. L.; Yan, J. *IEEE Trans. Electron Devices* **1997**, *44*, 104.
(2) Jones, R. E., Jr.; Zurcher, P.; Chu, P.; Taylor, D. J.; Lii, Y. T.; Jiang, B.; Maniar, P. D.; Gillespie, S. J. *Microelectron. Eng.* **1995**, *29*, 3.
(3) Peng, C. H.; Desu, S. B. *J. Am. Ceram. Soc.* **1994**, *77*, 1799.
(4) Cava, R. F.; Peck, W. F., Jr.; Krajewski, J. J. *Nature (London)* **1995**, *377*, 215.
(5) Rees, W. S. Jr., Ed. *CVD of Nonmetals*; VCH Verlagsgesellschaft mbH and VCH Publishers: Weinheim, Germany, and New York, 1996.
(6) Lee, J.-H.; Rhee, S.-W. *J. Mater. Res.* **1999**, *14*, 3988.
(7) Lee, J.-H.; Rhee, S.-W. *J. Electrochem. Soc.* **1999**, *146*, 3783.
(8) Scott, J. F.; Kammerdiner, L.; Parris, M.; Traynor, S.; Ottenbacher, V.; Shawabkeh, A.; Oliver, W. F. *J. Appl. Phys.* **1988**, *64*, 787.
(9) Horikawa, H.; Mikami, N.; Makita, T.; Tanimura, J.; Kataoka, M.; Sato, K.; Nunoshita, M. *Jpn. J. Appl. Phys.* **1993**, *32*, 4126.
(10) Kang, C. S.; Cho, H. J.; Lee, B. T.; Lee, K. H. *Jpn. J. Appl. Phys.* **1997**, *36*, 6946.

10.1021/ic0256967 CCC: $25.00
Published on Web 02/20/2003

ytetramethylheptanedionate) are reported to yield BST films with constant Ba and Sr composition ratios via deposition at 400−600 °C.[9,10] To avoid diffusion problems and to obtain good step coverage and surface uniformity, a typical high-density semiconductor process requires low-temperature deposition. For the application of BST films in DRAM capacitors, the desirable deposition temperature is in the range 400−480 °C. It follows that the ideal Ti precursor must undergo complete decomposition within this low-temperature range while remaining stable at the temperature of the vaporization process (ca. 280 °C).

To date, several Ti precursors have been tested for the deposition of BST films. The ubiquitous titanium tetrachloride ($TiCl_4$) and titanium tetraalkoxide [$Ti(OR)_4$, R = alkyl] precursors have several drawbacks in BST film deposition.[1,3,11−13] $TiCl_4$ requires a deposition temperature above 500 °C and, moreover, leaves chloride impurities in the film. Titanium tetraalkoxides are moisture-sensitive and are apt to prereact in the gas phase before film deposition. These problems conspire to complicate control of the BST film composition. The most popular Ti precursors developed so far are $Ti(OPr^i)_2(tmhd)_2$ and $Ti(mpd)(tmhd)_2$ (mpd = 2-methyl-2,4-pentanediolate). The introduction of tmhd instead of alkoxide saturates the coordination sphere of titanium, improves the thermal stability, and lowers the moisture sensitivity.[14,15] However, these precursors also have disadvantages. At a deposition temperature below 480 °C, the precursor decomposition is incomplete, and Ti is poorly incorporated into the BST film. It is believed that the strong bonding between Ti and tmhd makes complete thermal decomposition difficult, which is manifested as Ti deficiency, or an irregular and hazy appearance of the BST film.[9,16−19] The titanium complex of the functionalized alkoxide $Ti(dmae)_4$ (dmae = dimethylaminoethoxide) was reported to have better deposition properties compared to those of simple alkoxide complexes, but moisture sensitivity and prereaction in the gas phase remained problematic.[16,20]

It would appear that the Ti−alkoxide bond is too weak and the Ti−tmhd bond is too strong to allow satisfactory control of the Ti composition in BST films formed in the temperature range 400−480 °C. The introduction of a monoanionic chelating ligand having a slightly weaker bond with Ti than Ti-tmhd bond and, at the same time, having a stronger bond with Ti than T-alkoxide could be a good choice for the design of a better Ti precursor. Consideration of the resonance-stabilized structures of tmhdH and the tmhd−Ti fragment shown in Figure 1 suggests that a monoanionic chelating ligand such as a β-ketoester would make a slightly weaker bond with Ti, which, in turn, would lead to a higher deposition rate. We chose mdop [$(CH_3)_3CC(O)C^-HCOOCH_3$] as a monoanionic chelating ligand to test our reasoning. Herein, we report the synthesis of the Ti precursors $Ti(mpd)(mdop)_2$ (**1**) and $[Ti(mpd)(mdop)(\mu\text{-OMe})]_2$ (**2**), which are air-stable and feature much higher deposition rates than $Ti(OPr^i)_2(tmhd)_2$ and $Ti(mpd)(tmhd)_2$ within the temperature range 400−475 °C.

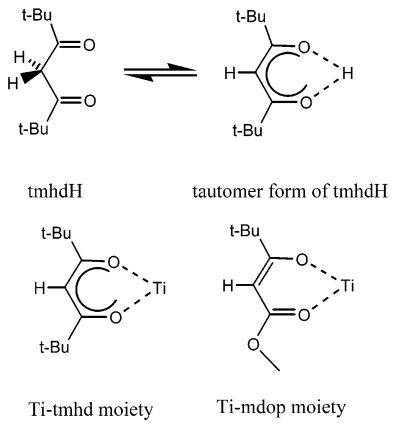

Figure 1. Structures of a tautomer form of tmhdH and the Ti−tmhd and Ti−mdop moieties.

Experimental Section

General Procedures. All operations were performed in an inert atmosphere using Schlenk techniques. *n*-Hexane was distilled under nitrogen from sodium benzophenone ketyl. Methanol was treated with Linde-type 4 Å molecular sieves and then distilled. $Ti[OCH(CH_3)_2]_4$ (Junsei Chemical Co., Ltd, guaranteed reagent) and methyl 4,4-dimethyl-3-oxopentanoate (mdopH; Aldrich, 99%) were used as purchased. 2-Methyl-2,4-pentanediol ($mpdH_2$; Aldrich, 99%) was refluxed with CaH_2 and then distilled.[21]

The characterization of the synthesized complexes was performed by ^1H NMR and ^{13}C NMR (INOVA 600, unitynmr600), FT-IR (Nicolet Magna 750), and mass spectroscopy (Finnigan LCQ, benzene solution, APCI or ESI). Melting points were measured with an electrothermal melting-point apparatus. Elemental analyses were performed by the Advanced Analytical Center in the Korea Institute of Science and Technology. Thermal analysis was carried out with model TA2960 TGA/DTA, with a heating rate of 10 °C/min in a nitrogen purge.

Synthesis of 1. A total of 4.72 mL (16.0 mmol) of $Ti[OCH(CH_3)_2]_4$ was dissolved in 16 mL of *n*-hexane, and 2.04 mL (16.0 mmol) of $mpdH_2$ was added with continuous stirring. After 1 h, 5.11 mL (32.0 mmol) of mdopH was added to the solution, which was stirred overnight at room temperature. The hexane solvent and byproduct 2-propanol were stripped off, and compound **1** was separated as a sticky, yellow liquid by fractional distillation under reduced pressure. Bp: 150 °C/0.4 mmHg. Yield: 6.48 g (84.7%). Complex **1** consists of two stereoisomers in solution. The ^1H NMR spectrum at 4 °C was very similar to that at 25 °C except for

(11) Akhtar, M. K.; Pratsinis, S. E.; Mastrangelo, S. V. R. *J. Mater. Res.* **1994**, *9*, 1241.
(12) Yeung, K. S.; Lam, Y. W. *Thin Solid Films* **1983**, *109*, 169.
(13) Takahashi, Y.; Tsuda, K.; Sugiyama, K.; Minoura, H.; Makino, D.; Tsuiki, M. *J. Chem. Soc., Faraday Trans.* **1981**, *77*, 1051.
(14) Akutsu, M.; Kubota, N.; Masuko, S.; Yamada, N. Jpn. Patent 10114781.
(15) Sato, Y. Jpn. Patent 11255784.
(16) Lee, J.-H.; Kim, J.-Y.; Shim, J.-Y.; Rhee, S.-W. *J. Vac. Sci. Technol., A* **1999**, *17*, 3033.
(17) Lee, J.-H.; Kim, J.-Y.; Rhee, S.-W. *Electrochem. Solid-State Lett.* **1999**, *2*, 507.
(18) Gao, Y.; Perkins, C. L.; He, S.; Alluri, P.; Tran, T.; Thevuthasan, S.; Henderson, M. A. *J. Appl. Phys.* **2000**, *87*, 7430.
(19) Kiyotoshi, M.; Eguchi, K.; Imai, K.; Arikado, T. *Jpn. J. Appl. Phys.* **1998**, *37*, 4487.
(20) Jones, A. C.; Leedham, T. J.; Wright, P. J.; Crosbie, M. J.; Fleeting, K. A.; Otway, D. J.; O'Brien, P.; Pemble, M. E. *J. Mater. Chem.* **1998**, *8*, 1773.
(21) Armarego, W. L. F.; Perrin, D. D. *Purification of Laboratory Chemicals*; Butterworth-Heinemann: Oxford, U.K., 1996.

improved sharpness. The rapid interconversion of the two isomers led to overlapping and partially resolved peaks on the NMR time scale. ^{1}H NMR (600 MHz, two isomers in C_6D_6 at 25 °C) δ: 1.214 & 1.225 [s each, 18H, C(C*H*$_3$)$_3$], 1.133 & 1.311 [s each, 6H, $CH_2C(O^-)(CH_3)_2$], 1.433 & 1.600 [s each, 3H, $CH_3C(O^-)HCH_2C(O^-)$], 1.841 & 1.818 [d each, J = 2 Hz, 1H, $CH_3C(O^-)HCH_2C(O^-)$], 2.000 & 2.034 [t each, J = 12 Hz, 1H, $CH_3C(O^-)HCH_2C(O^-)$], 3.234 & 3.264 [s each, 6H, $COOCH_3$], 4.983 & 5.175 [br each, 1H, $CH_3C(O^-)HCH_2C(O^-)$], 5.314 & 5.333 [s each, 2H, $C(O)C^-HCOOCH_3$]. ^{13}C{^{1}H} NMR (600 MHz, two isomers in C_6D_6 at 25 °C) δ: 23.87 & 24.03 [$CH_2C(O^-)(CH_3)_2$], 27.17 & 27.34 [$CH_3C(O^-)HCH_2$], 28.35 & 28.42 [$(CH_3)_3CCO$], 31.46 & 31.52 [$CH_3C(O^-)HCH_2C(O^-)$], 39.54 & 39.67 [$(CH_3)_3CCO$], 51.47 [$C(O)C^-HCOOCH_3$], 53.30 & 53.60 [$COOCH_3$], 77.80 & 78.14 [$CH_2C(O^-)(CH_3)_2$], 84.44 & 84.76 [$CH_3C(O^-)HCH_2$], 174.83 & 174.94 [$COOCH_3$], 194.61 & 194.74 [$(CH_3)_3CCO$]. FT-IR (in benzene, cm^{-1}): 1629, 1612, 1590 (CO stretching), 1534, 1508 (C═C stretching). MS: 478 (100%, M), 464 (17%), 338 (17%). Elem anal. Calcd for $C_{22}H_{38}O_8Ti$: C, 55.2; H, 8.0. Found: C, 55.4; H, 8.1.

Synthesis of 2. The procedure for the synthesis of **1** was repeated up to the stage of removing the solvent and byproduct 2-propanol. Then, 8 mL of dried methanol was added to give a white precipitate, which was separated by filtration. The filtrate was concentrated and kept in a refrigerator to yield more solid. The combined solids were dried overnight in a vacuum. The solid product was characterized as complex **2**. Mp: 139−142 °C (not corrected). Yield: 4.98 g (65%). Compound **2** consists of several stereoisomers in solution but crystallizes in a single stereoisomer. ^{1}H NMR (600 MHz, several isomers in C_6D_6) δ: 1.116−1.324 [several s, 30H, C(C*H*$_3$)$_3$ and $CH_2C(O^-)(CH_3)_2$], 1.445−1.614 [several s, 6H, $CH_3C(O^-)HCH_2C(O^-)$], 1.682−1.835 [several d, 2H, $CH_3C(O^-)HCH_2C(O^-)$], 1.852−2.690 [several t, 2H, $CH_3C(O^-)HCH_2C(O^-)$], 3.232 & 3.263 [s each, 6H, $COOCH_3$], 3.676−3.774 [several s, 3H, μ-OCH_3], 4.413−4.469 [several s, 3H, μ-OCH_3], 4.583−5.193 [several br, 2H, $CH_3C(O^-)HCH_2C(O^-)$], 5.533−5.417 [several s, 2H, $C(O)C^-HCOOCH_3$]. ^{13}C{^{1}H} NMR (600 MHz, several isomers in C_6D_6, several closely spaced peaks appeared at each resonance position) δ: 23.88−24.65 [$CH_2C(O^-)(CH_3)_2$], 27.19−27.75 [$CH_3C(O^-)HCH_2$], 28.36−28.59 [$(CH_3)_3CCO$], 31.48−32.12 [$CH_3C(O^-)HCH_2C(O^-)$], 39.39−39.67 [$(CH_3)_3CCO$], 51.49−52.29 [$C(O)C^-HCOOCH_3$], 53.34−53.81 [$COOCH_3$], 61.45−62.55 (μ-OCH_3), 75.50−76.31 (μ-OCH_3), 77.77, 78.05, & 78.11 [$CH_2C(O^-)(CH_3)_2$], 84.23−85.19 [$CH_3C(O^-)HCH_2$], 174.36−174.80 [$COOCH_3$], 193.73−194.70 [$(CH_3)_3CCO$]. IR (in C_6D_6, cm^{-1}): 1632, 1594 (CO stretching), 1535, 1511 (C═C stretching). MS: 673 (8%, M − OCH_3^-), 619 (26%), 575 (35%), 521 (31%), 480 (100%), 440 (88%), 394 (79%), 353 (44%). Elem anal. Calcd for $C_{30}H_{56}O_{12}Ti_2$: C, 51.1; H, 8.01. Found: C, 51.4; H, 8.05.

Crystal Structure Determination. A colorless crystal of **2** with dimensions 0.40 × 0.28 × 0.24 mm^3 was attached to the tip of a glass fiber, transferred to a Bruker SMART diffractometer/charge-coupled device (CCD) area detector, and centered under liquid nitrogen in the beam at 233(2) K. The crystal evaluation and data collection were performed on a Bruker CCD diffractometer with Mo Kα (λ = 0.710 73 Å) radiation, employing a 2-kW sealed-tube X-ray source operating at 1.6 kW and diffractometer-to-crystal distance of 4.9701 cm. The preliminary orientation matrix and cell constants were determined from three series of ω scans at different starting angles. Each series consisted of 10 frames collected at intervals of 0.3° with the exposure time of 10 s per frame. The reflections were successfully indexed by an automated indexing routinely built in the SMART program.[22a] A total of 14 278 data were harvested by collecting three sets of frames with 0.3° ω scans with an exposure time of 10 s per frame. The highly redundant data sets were corrected for Lorentz and polarization effects. The structure was solved by the application of direct methods[22b] and least-squares refinement using SHELXL-97.[22c] After the anisotropic refinement of all non-hydrogen atoms, several hydrogen-atom positions could be located in difference Fourier maps. These were refined isotropically while the remaining hydrogen atoms were calculated in idealized positions and included in the refinement with fixed atomic contributions. Further detailed information is listed in Table 1.

Table 1. X-ray Crystallographic Data for Complex **2**

chemical formula	$C_{30}H_{56}O_{12}Ti_2$
fw	704.57
temp	233(2) K
wavelength	0.710 73 Å
cryst syst, space group	monoclinic, $P2_1/c$
unit-cell dimensions	a = 12.570(4) Å; α = 90°
	b = 13.817(4) Å; β = 101.059(5)°
	c = 11.157(3) Å; γ = 90°
vol	1901.8(10) Å^3
Z	2
D_{calcd}	1.140 g/cm^3
μ	0.463 mm^{-1}
final R indices [$I > 2\sigma(I)$]	$R_1{}^a$ = 0.0744, $wR_2{}^b$ = 0.2281
R indices (all data)	$R_1{}^a$ = 0.1026, $wR_2{}^b$ = 0.2460

^{a} $R_1 = \sum||F_o| - |F_c||$ (based on reflections with $F_o^2 > 2\sigma F^2$). ^{b} $wR_2 = \{\sum[w(F_o^2 - F_c^2)^2]/\sum[w(F_o^2)^2]\}^{1/2}$; $w = 1/[\sigma^2(F_o^2) + (0.095P)^2]$; $P = [\max(F_o^2, 0) + 2F_c^2]/3$ (also with $F_o^2 > 2\sigma F^2$).

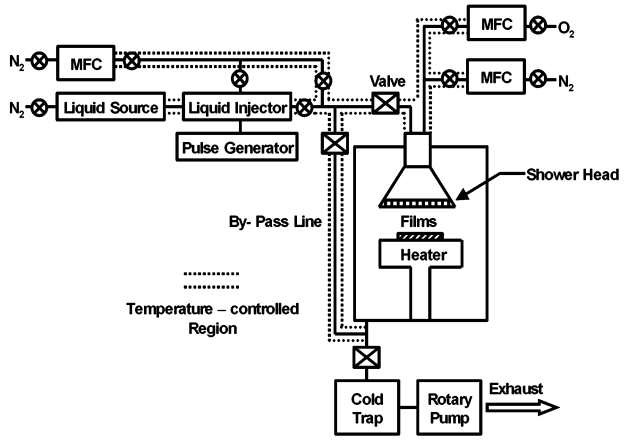

Figure 2. Schematic diagram of the LS-MOCVD system for TiO_2 film deposition.

Fabrication of TiO_2 Thin Films. The MOCVD of TiO_2 films using a direct liquid-injection method with a flash vaporizer was carried out with compounds **1** and **2** and $Ti(OPr^i)_2(tmhd)_2$ and Ti(mpd)(tmhd)$_2$ as precursors on the substrate of Pt/Ti/SiO_2/Si. The liquid-source (LS)-MOCVD system is described in Figure 2, and the detailed LS-MOCVD conditions are provided in Table 2. The chemical composition of the films as a function of thickness was examined by Auger electron spectroscopy/scanning Auger electron microscopy (performed by the Advanced Analytical Center in the Korea Institute of Science and Technology). X-ray diffraction (XRD) patterns were obtained with a Philips diffractometer (PW3020) using a monochromated high-intensity Cu Kα radiation. The surface morphology and film thickness were measured via scanning electron microscopy (SEM; Hitachi S-4500).

(22) (a) *SMART: Area-Detector Software Package*, Bruker AXS, Inc.: Madison, WI, 1995. (b) Sheldrick, G. M. *Acta Crystallogr., Sect. A* **1990**, *A46*, 467. (c) Sheldrick, G. M. *SHELXL: Program for Crystal Structure Refinement*; University of Göttingen: Göttingen, Germany, 1997.

Table 2. Typical Deposition Conditions for the LS-MOCVD of TiO_2 Thin Films

compound **1** in toluene	0.08 mol/L	0.1 mL/min
compound **2** in toluene	0.04 mol/L	0.1 mL/min
$Ti(mpd)(tmhd)_2$ in *n*-butyl acetate	0.08 mol/L	0.1 mL/min
$Ti(OPr^i)_2(tmhd)_2$ in *n*-butyl acetate	0.08 mol/L	0.1 mL/min

oxidizer (O_2/N_2) flow rate	97/277 mL/min
carrier (N_2) flow rate	112 mL/min
substrate temp	375−475 °C
vaporizer temp	280 °C
line heating temp	250 °C
reactor pressure	2 Torr

Scheme 1. Synthetic Procedure for Complexes **1** and **2**

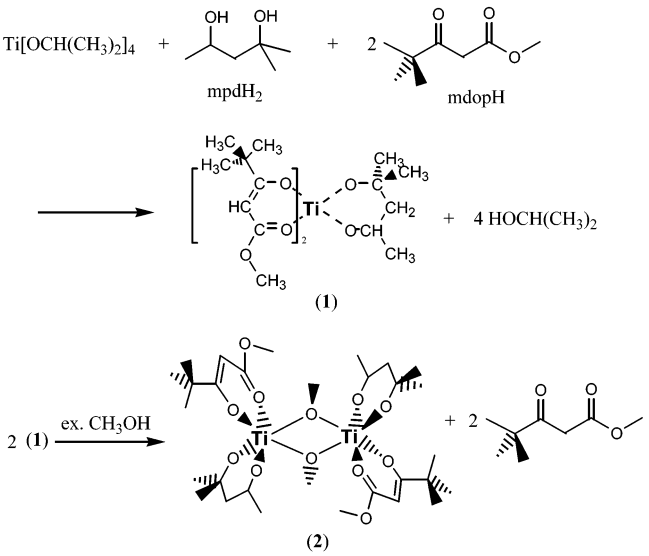

Results and Discussion

As a result of inductive and possible resonance effects (vide infra), we reasoned that a β-ketoester, rather than a β-diketone, should have a weaker bond to Ti. A weaker Ti−ligand bond would imply a higher deposition rate of TiO_2 thin films. Accordingly, we decided to investigate the properties of the Ti−mdop moiety (Figure 1). Complex **1** was easily synthesized and was found to react with excess methanol to yield the dimeric complex **2**, as indicated in Scheme 1.

The molecular formula of the oily compound **1** was characterized as $Ti(mpd)(mdop)_2$ from NMR, IR, elemental, and mass spectroscopic analyses. Complex **1** is coordinatively saturated by three bidentate ligands and assumed to be monomeric from the result of mass spectroscopy. The mass spectrum of **1** showed negligible intensity above the molecular weight ($M^+ = 478$, 100%) of the monomer. The ^1H NMR spectrum of **1** was clean and indicated the presence of two stereoisomers in similar abundance. The proton-decoupled ^{13}C NMR spectrum of **1** showed two peaks closely spaced at each resonance position, again indicating the existence of two stereoisomers. The FT-IR spectrum of **1** showed the C═O stretching bands of the chelated mdop at 1629, 1612, and 1590 cm^{-1}, which are shifted about 120 cm^{-1} from those of free mdopH. Bands present at 1534 and 1508 cm^{-1} are believed to be due to the C═C stretching modes of the mdop chelate ring. Although complex **1** is volatile and could be distilled under reduced pressure, it could only be obtained as a yellow, sticky oil and was rather inconvenient to handle. In an effort to prepare **1** in a more convenient form, several solvent systems were utilized. During the course of this, it was found that dry methanol rapidly converts **1** to the dimer **2**. It is quite interesting that methoxide can substitute for an mdop ligand and can make a bridged complex. Further study is required to understand the mechanism of this substitution.

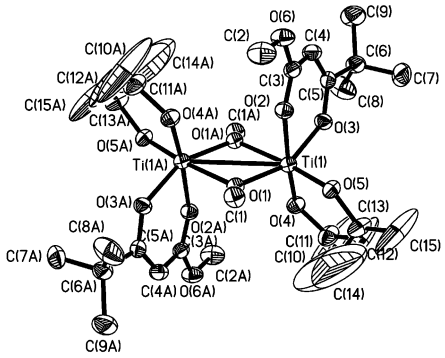

Figure 3. Representation of the X-ray crystal structure of complex **2**, showing a 30% probability of thermal ellipsoids.

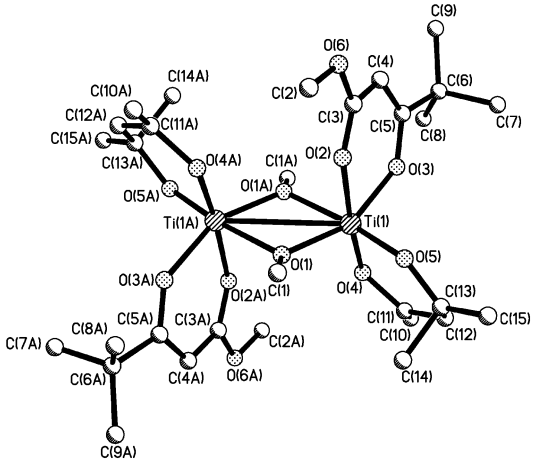

Figure 4. Ball-and-stick representation of the X-ray crystal structure of complex **2**.

The ^1H NMR spectrum of **2** was complicated because of the existence of several stereoisomers. The same ^1H NMR spectral pattern was obtained from a single crystal of **2** used for X-ray structural analysis. The proton-decoupled ^{13}C NMR spectrum showed several very closely spaced peaks at each resonance position, indicating the existence of several stereoisomers. The IR spectrum of **2** was similar to that of **1**. Mass spectroscopy showed an $M-OCH_3^-$ peak at the highest mass-to-charge ratio, 673. The elemental C and H analyses agreed well with the proposed molecular formula for **2**.

The crystal structure of **2** is shown in Figure 3, and a ball-and-stick representation is provided in Figure 4. Selected bond lengths and angles are collected in Tables 3 and 4. Complex **2** exists as a dimer connected through two methoxy bridges in the solid state, and the two molecular units comprising the dimer are each constrained by a crystallographic center of inversion. The Ti_2O_2 core is coplanar because of its symmetry, with the interatomic bond angles

Table 3. Selected Interatomic Bond Lengths (Å) for Complex **2**[a]

Ti(1)−O(5)	1.807(3)	Ti(1)−O(4)	1.809(3)
Ti(1)−O(3)	1.968(3)	Ti(1)−O(1)	1.969(3)
Ti(1)−O(1A)	2.075(3)	Ti(1)−O(2)	2.121(3)
Ti(1)−Ti(1A)	3.2450(18)	O(1)−C(1)	1.420(5)
O(2)−C(3)	1.247(5)	O(4)−C(11)	1.432(6)
O(3)−C(5)	1.291(6)	O(5)−C(13)	1.411(6)
C(5)−C(4)	1.375(7)	C(3)−C(4)	1.390(6)
C(11)−C(12)	1.457(9)	C(13)−C(12)	1.379(9)

[a] Symmetry transformations used to generate equivalent atoms: (1A) $-x+2, -y+2, -z$.

Table 4. Selected Bond Angles (deg) for Complex **2**[a]

O(5)−Ti(1)−O(4)	91.42(14)	O(5)−Ti(1)−O(3)	99.63(15)
O(4)−Ti(1)−O(3)	93.57(14)	O(5)−Ti(1)−O(1)	97.53(14)
O(4)−Ti(1)−O(1)	103.24(13)	O(3)−Ti(1)−O(1)	155.59(14)
O(5)−Ti(1)−O(1A)	170.75(13)	O(4)−Ti(1)−O(1A)	92.02(13)
O(3)−Ti(1)−O(1A)	88.72(13)	O(1)−Ti(1)−O(1A)	73.32(13)
O(5)−Ti(1)−O(2)	87.85(13)	O(4)−Ti(1)−O(2)	174.49(13)
O(3)−Ti(1)−O(2)	81.17(13)	O(1)−Ti(1)−O(2)	82.27(12)
O(1A)−Ti(1)−O(2)	89.52(11)	O(5)−Ti(1)−Ti(1A)	135.29(11)
O(4)−Ti(1)−Ti(1A)	99.30(11)	O(3)−Ti(1)−Ti(1A)	122.57(10)
O(1)−Ti(1)−Ti(1A)	37.77(9)	O(1A)−Ti(1)−Ti(1A)	35.55(8)
O(2)−Ti(1)−Ti(1A)	85.01(9)	Ti(1)−O(1)−Ti(1A)	106.68(13)

[a] Symmetry transformations used to generate equivalent atoms: (1A) $-x+2, -y+2, -z$.

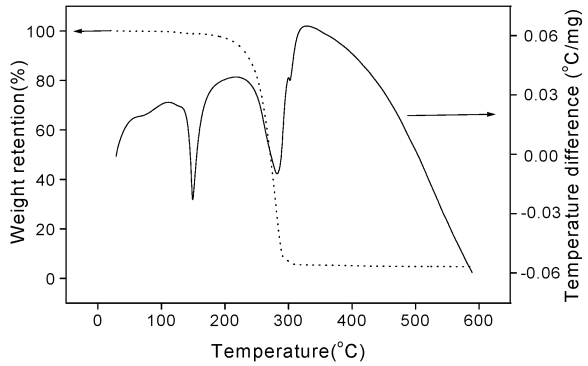

Figure 5. Thermal-analysis curve of complex **2** with a heating rate of 10 °C/min under nitrogen.

being O(1)−Ti(1)−O(1A) = 73.32(13)° and Ti(1)−O(1)−Ti(1A) = 106.68(13)°. The Ti(1)−O(3), O(3)−C(5), and C(5)−C(4) and Ti(1)−O(2), O(2)−C(3), and C(3)−C(4) bond lengths are 1.968(3), 1.291(6), and 1.375(7) and 2.121(3), 1.247(5), and 1.390(6) Å, respectively, indicating a higher contribution of the enolate form of the ketone moiety to the bonding compared to that of the ester moiety. The longer Ti(1)−O(2) bond length implies a weaker interaction between Ti and the ester end of mdop. On the other hand, in the case of the Ti−tmhd moiety, the same high contribution is expected from the two enolate forms of tmhd. This is believed to be the origin of the stronger Ti−tmhd bond. This difference in bonding is reflected in different deposition rates, as will be shown.

The result of a thermal analysis of **2** is shown in Figure 5. The differential thermal-analysis curve indicates that the melting point and boiling point of complex **2** are about 150 and 280 °C, respectively. It is suggested that the shoulder at about 300 °C is due to the thermal decomposition. No additional peaks were found above 300 °C. At the same time, no appreciable weight change is observed from the thermogravimetric thermogram. This indicates that complete decomposition is achieved at very low temperature, and the decomposition mechanism of **2** is a simple one-step process. The residual sample after programmed heating in a nitrogen environment was less than 4%. Thus, it is suggested that **2** is stable during the flash-evaporation process. The thermal behavior of compound **1** (not shown here) was similar to that of **2** above 300 °C, which is to be expected because they have common Ti−ligand bonds.

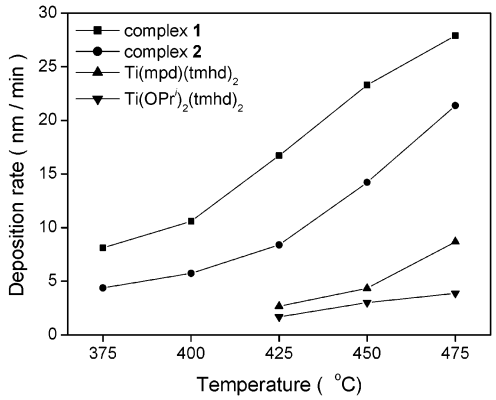

Figure 6. Deposition rate of TiO_2 films at various deposition temperatures; $Ti(mpd)(tmhd)_2$ and $Ti(OPr^i)_2(tmhd)_2$ (0.08 M) in *n*-butyl acetate at 280 °C and **1** and **2** (0.08 M) in toluene at 280 °C.

The precursors **1** and **2** are stable in air and solvents such as tetrahydrofuran and toluene. The solubilities of compounds **1** and **2** in these solvents are adequate for LS-MOCVD.

The deposition rate of TiO_2 thin films with precursors **1** and **2** was monitored as a function of the deposition temperature, as shown in Figure 6. The vaporization temperature was adjusted to 280 °C on the basis of differential thermal analysis data. After several runs, there was no residue on the vaporizer. In comparison, $Ti(mpd)(tmhd)_2$ and $Ti(OPr^i)_2(tmhd)_2$ were also tested for the deposition of TiO_2 thin films. The deposition rates with precursors **1** and **2** are 17−28 and 9−24 nm/min, more than 3 times higher than that with $Ti(mpd)(tmhd)_2$ in a range of 425−475 °C. Compared to that of $Ti(OPr^i)_2(tmhd)_2$, the deposition rates of **1** and **2** are approximately 5−6 times higher. It was found that the high deposition rate of TiO_2-film formation from **1** and **2** was obtainable even at a temperature as low as 375 °C.

We conclude that a β-ketoester ligand makes a weaker bond to Ti than the corresponding β-diketone ligand and that the weaker Ti−ligand bond allows for a higher deposition rate. A similar observation has been recently reported by Chen et al.,[23] who found that copper precursors with β-diketone ligands needed a higher deposition temperature than those with β-ketoester ligands.

Complex **1**, as a result of its sticky, oily nature, is inconvenient as a precursor, and, consequently, further characterizations were performed only for films fabricated from complex **2**.

Figure 7 shows the Auger depth profile of a TiO_2 film of 140-nm thickness, obtained from a 5-min deposition at 450

(23) Chen, T.-Y.; Vaissermann, J.; Ruiz, E.; Senateur, J. P.; Doppelt, P. *Chem. Mater*. **2001**, *13*, 3993.

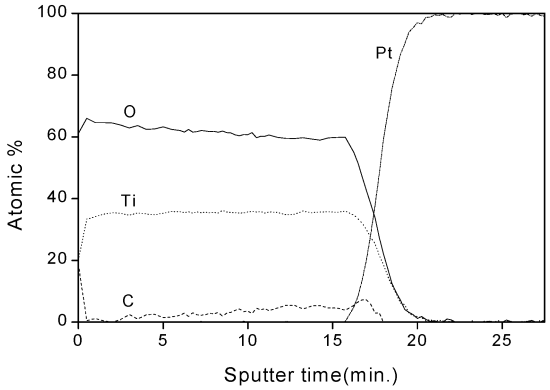

Figure 7. Auger depth profile of TiO_2 film deposited on the Pt/Ti/SiO_2/Si substrate from complex **2** at a deposition temperature of 450 °C.

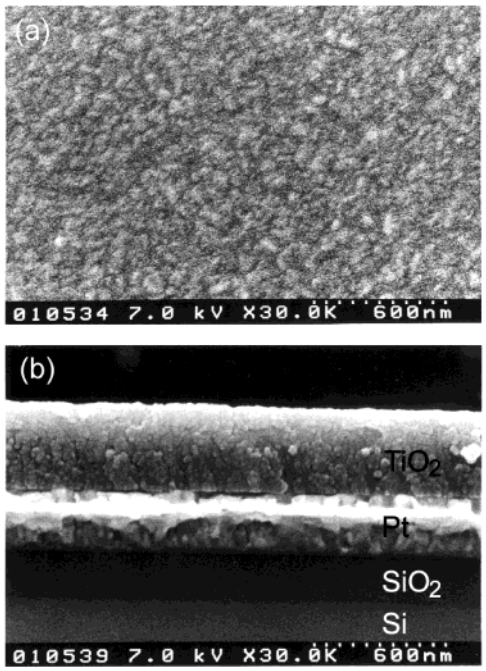

Figure 8. (a) Plane-view and (b) cross-sectional-view SEM photographs of TiO_2 film deposited from complex **2** at 450 °C.

°C using complex **2**. The calculated composition of the film is TiO_2, and the carbon content in the as-deposited film is below 3%. The field emission SEM images in Figure 8 show the plane view and cross-sectional view of a fabricated TiO_2 film. The grains are nanosized, and the films show a uniform smooth surface without any bumps or a hazy appearance. Figure 9 shows the XRD pattern of the film prepared from compound **2** at 450 °C. The film is relatively well-crystallized compared with those obtained by other commercial Ti precursors (Supporting Information). The peak intensity and

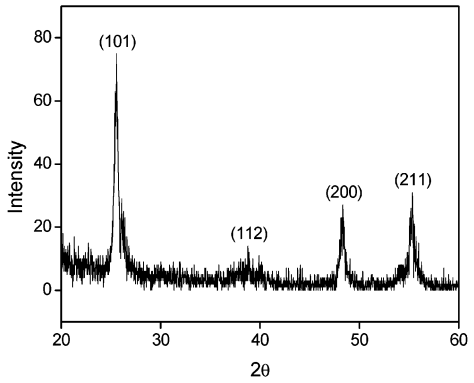

Figure 9. XRD pattern of TiO_2 film deposited from complex **2** at 450 °C.

position of the film match well with those of TiO_2 in the anatase phase from standard JCPDS data.[24]

Further study is in progress to investigate the compatibility of compound **2** with commercial Ba and Sr precursors for the fabrication of BST thin films.

Conclusion

The synthesis and application of the novel Ti precursors **1** and **2** for the LS-MOCVD of TiO_2 thin films were studied. Both precursors are volatile, air stable, and thermally stable. Complex **2** is a white solid, while **1** is a sticky, oily liquid. The deposition rates with complexes **1** and **2** are much higher than those with Ti(mpd)(tmhd)$_2$ or Ti(OPr^i)$_2$(tmhd)$_2$. The higher deposition rates can be attributed to a weaker bonding to Ti from an ester moiety compared to that from a ketone moiety. A high deposition rate of TiO_2-film formation was obtainable at temperatures as low as 375 °C. TiO_2 thin films made from complex **2** were crystalline and showed low carbon content with a smooth surface morphology. It is concluded that **2** will prove to be a good LS-MOCVD precursor.

Acknowledgment. This research has been conducted under the KIST-2000 program sponsored by the Ministry of Science and Technology in Korea. The authors are grateful to Dr. Byungjoo Kim for mass data.

Supporting Information Available: The SEM images and XRD patterns of TiO_2 films fabricated from the other commercial precursors, the crystal data of complex **2**, and one X-ray crystallographic file in CIF format. Available free of charge via the Internet at http://pubs.acs.org.

IC0256967

(24) JCPDS-International Center for Diffraction Data, File No. 21-1272, 1995.